THE JOURNAL OF BIOLOGICAL CHEMISTRY
Vol. 276, No. 13, Issue of March 30, pp. 10234–10246, 2001

Printed in U.S.A.

The RepE Initiator Is a Double-stranded and Single-stranded DNA-binding Protein That Forms an Atypical Open Complex at the Onset of Replication of Plasmid pAMβ1 from Gram-positive Bacteria*

Received for publication, November 7, 2000
Published, JBC Papers in Press, December 20, 2000, DOI 10.1074/jbc.M010118200

Emmanuelle Le Chatelier, Laurent Jannière‡, S. Dusko Ehrlich, and Danielle Canceill§

From the Laboratoire de Génétique Microbienne, Institut National de la Recherche Agronomique, Domaine de Vilvert, 78350 Jouy en Josas, France

The RepE protein of the broad host range pAMβ1 plasmid from Gram-positive bacteria is absolutely required for replication. To elucidate its role, we purified the protein to near homogeneity and analyzed its interactions with different nucleic acids using gel retardation assays and footprinting experiments. We show that RepE is monomeric in solution and binds specifically, rapidly, and durably to the origin at a unique double-stranded binding site immediately upstream from the initiation site of DNA replication. The binding induces only a weak bend (31°). Unexpectedly, RepE also binds nonspecifically to single-stranded DNA with a 2–4-fold greater affinity than for double-stranded origin. On a supercoiled plasmid, RepE binding to the double-stranded origin leads to the denaturation of the AT-rich sequence immediately downstream from the binding site to form an open complex. This open complex is atypical since (i) its formation requires neither multiple RepE binding sites on the double-stranded origin nor strong bending of the origin, (ii) it occurs in the absence of any cofactors (only RepE and supercoiling are required), and (iii) its melted region serves as a substrate for RepE binding. These original properties together with the fact that pAMβ1 replication depends on a transcription step through the origin on DNA polymerase I to initiate replication and on a primosome to load the replisome suggest that the main function of RepE is to assist primer generation at the origin.

DNA replication is carried out by the replisome, a multiprotein complex able to carry on strand separation, primer synthesis, and a rapid, accurate, and concerted synthesis of the continuous and discontinuous strands. At the onset of replication, replisome assembly is generally orchestrated by a protein or a multiprotein complex called initiator. The initiator recognizes and binds specific or preferential sites in DNA molecules (the origin), melts these regions by causing a structural distortion of the DNA, and initiates the loading of the replisome through protein-protein interactions.

The most thoroughly characterized initiator is the *Escherichia coli* DnaA protein, which possesses conserved homologues in all known bacteria (see for review Ref. 1). Various properties have been attributed to DnaA, such as sequence-specific DNA binding, oligomerization, protein-protein interactions, membrane binding, ATP and ADP binding, and ATPase activity (1, 2). At the onset of chromosome replication, the ATP-bound form of DnaA binds as a monomer to the chromosomal origin at five 9-bp[1] repeated sequences called DnaA boxes. It then oligomerizes to form a large nucleoprotein structure containing 20–40 DnaA molecules. The structure confers single-stranded character to a flanking AT-rich region (13-mer), forming an intermediate termed the open complex (3). The process requires negative supercoiling, either IHF or HU, and is activated by transcription and possibly by a direct interaction between DnaA and the AT-rich region (4). DnaA, with the help of DnaC, then recruits the host DNA helicase DnaB to the exposed single-stranded region. DnaB enlarges the unwound region and subsequently loads alone or together with DnaA the primase DnaG and the DNA polymerase III (3, 5–7).

Initiators of plasmid and viral θ replicons, form, like DnaA, an open complex at their cognate origins to recruit the replisome (8–10). Open complex formation occurs via specific binding of the initiator to repeated sequences (the iterons), oligomerization of the initiator, and eventually local DNA distortions such as bending, untwisting, or wrapping. However, this formation generally also requires DnaA and the help of cofactors including structural proteins (IHF, Fis, HU, SSB) or structural DNA determinants (intrinsically bent DNAs, AT-rich regions, sequences of natural instability such as DNA unwinding elements, or supercoiling of the DNA; reviewed in Refs. 11 and 12). Aside from the apparent consensual role of the initiators in origin binding and denaturation, variations occur in their ability to participate in steps after open complex formation. Some initiators (but not all) act similarly to DnaA, as a "landing pad" for replisome assembly. For instance, the UL9 initiator of herpes simplex virus-1 interacts with the cellular DNA polymerase-α primase, the helicase-primase complex, and the processivity polymerase factor (13). Likewise, the plasmid initiators π of R6K and RepA of pSC101 are known or supposed to interact with DnaA, the replicative helicase DnaB, the primase DnaG, and the τ subunit of DNA polymerase III (14–16). Initiators can also be helicases (T-antigen of simian virus 40 (17), UL9 of herpes simplex virus-1 (18), or E1 protein of

* The costs of publication of this article were defrayed in part by the payment of page charges. This article must therefore be hereby marked "*advertisement*" in accordance with 18 U.S.C. Section 1734 solely to indicate this fact.

‡ This author is from the CNRS staff.

§ To whom correspondence should be addressed. Tel.: 33-1 34 65 25 12; Fax: 33-1 34 65 25 21; E-mail: canceill@biotec.jouy.inra.fr.

[1] bp, base pair(s); BSA, bovine serum albumin; CBD, chitin binding domain; DMS, dimethyl sulfate; dsDNA, double-stranded DNA; ssDNA, single-stranded DNA; DTT, dithiothreitol; nt, nucleotide(s); OP-Cu, 1,10-orthophenanthroline-copper; *ori*, replication origin; Pol I, DNA polymerase I; RNA pol, RNA polymerase; PAGE, polyacrylamide gel electrophoresis; PCR, polymerase chain reaction; Bicine, *N*,*N*-bis(2-hydroxyethyl)glycine; ORC, origin recognition complex.

papillomavirus (19)), whereas others are primases (Rep of ColE2 (20)) or seem to have no extra activities apart from origin binding, bending, and melting (TrfA of RK2 (21)).

θ replicons that do not code for any initiator protein are a noticeable exception to this general scheme. They still initiate DNA replication at preferential sites, but these origins do not carry the relevant features usually found in the initiator-dependent replicons (see above). The initiation mechanism of these systems, such as the *E. coli* plasmid ColE1, phages T4, or T7 and the mitochondrial DNA of metazoans, mainly relies on the RNA polymerase (RNA pol), which provides the initial primer for DNA synthesis (22). In phage T7, RNA pol stops at the origin by an unknown mechanism, and the arrested transcript serves as a primer to initiate DNA synthesis. In ColE1, phage T4, and mitochondrial DNA replication, although RNA pol transcribes the origin, an R-loop is formed. The RNA strand of the R-loop is then processed by a RNaseH activity into the primer used to initiate leading strand synthesis. In ColE1, the primer is extended by Pol I, which unwinds the downstream region, leading to formation of D-loop structures, allowing, successively, recruitment of PriA or DnaABC primosomes and of full replisome (23, 24).

Another exception to the general scheme of initiation is plasmids of the pAMβ1 family from Gram-positive bacteria. Although they encode an initiator protein, they require for replication a small unstructured origin and a transcription step through the origin by the host RNA pol (25, 26). Furthermore, they are dependent on Pol I and independent of DnaA (25, 27, 28). The small origin (44 bp) does not possess some of the features found in other initiator-dependent plasmids, such as iterons, to allow binding of more than one monomer. However, it contains a 16-bp-long AT-rich region (88% AT against 68% for the whole origin). This AT-rich region is located immediately downstream from the initiation site of replication, itself located in the middle of the origin (29). The functions of both the transcription step and the initiator are unknown. The initiator, RepE, is a basic protein of 496 amino acids with no homologues in the data bases and no specific recognizable features (such as ATPase or helicase motives) other than a DNA binding motif (71% probability for a helix-turn-helix motif, according to the Dodd and Egan algorithm (30)) in the C-terminal region. The initial phase of pAMβ1 replication has been characterized to a certain extent. First, DNA replication is unidirectional. Second, mRNA originating upstream from the origin and synthesized codirectionally to DNA replication terminates at the initiation site of DNA replication, forming possible primers for leading strand synthesis (26). Third, the leading strand primer is used by Pol I to generate D-loop structures (~200 bp long) that are used as a signal for entry of the host PriA-dependent primosome (31–33).[2] It is thought that the primosome directs replisome assembly through the general mechanism of replication fork rescue (34). These observations provide some indirect information on RepE functions as follows. (i) RepE might recognize the origin and play a role in mRNA maturation, since mRNA ending at the initiation site requires the intact origin and an active RepE and (ii) RepE is an unlikely landing pad for replisome assembly, as this task seems to be ensured by the PriA-dependent primosome.

As a first step in unraveling how RepE functions, we purified it to near homogeneity and analyzed its interactions with different nucleic acids. Results show that RepE binding to *ori*-containing supercoiled molecules leads to formation of an open complex in which the 20–30 nt encompassing the initiation site of DNA replication and downstream sequences are melted. An unexpected strong and nonspecific ssDNA binding activity allows RepE to bind to the melted region of the open complex. These results, which describe for the first time an open complex at the origin of a θ-replicating plasmid from a Gram-positive bacterium, are discussed in terms of possible mode of action of RepE in pAMβ1 initiation mechanism.

EXPERIMENTAL PROCEDURES

Strains and Plasmids—The strains used were *E. coli* MC1061 (F^- *araD139* Δ*(ara-leu)7696 galE15 galK16* Δ*(lac)X74 rpsL* (Str^r) *hsdR* (r_K^- mK^+) *mcrA mcrB1*) and *Bacillus subtilis* 168, 1A224, and its isogenic *polA5* mutant, 1A226, which have been described previously (25). Plasmids pIL253, pHV1455, and pHV1455Rep* were described elsewhere (31, 33, 35).

To express and purify RepE, we constructed pCYB1*repE* using the pCYB1 vector (IMPACT I system from New England Biolabs), which allows the expression under the control of the Ptac promoter of a fusion between the C terminus of a target protein and the N terminus of a self-cleavable intein/chitin binding domain (CBD) tag. The *repE* open reading frame was amplified by PCR using pIL253 as substrate and the following primers: 5′-gagggaattccatATGAATATCCCTTTTGTTGT-3′ (containing an *Nde*I site, underlined) and 5′-ggaattcgctcttccgcaGCCT-GTATCATAGCTAAACAAATCG-3′ (containing a *Sap*I site). The PCR product was cloned into the *Nde*I and *Sap*I sites of pCYB1, allowing a precise fusion between the last Gly codon of RepE gene and the N terminus of the removable intein tag.

pBend2*ori* derives from pBend2 (36) by insertion of the minimal 44-bp pAMβ1 *ori* in the *Sal*I site of the polylinker, such as pAMβ1 replication would proceed in the direction of the ampicillin gene.

pGEM*ori* mainly derives from pGEM-3Zf+ (Promega) by insertion of a pAMβ1 49-bp *ori* segment in the *Eco*RI site of the polylinker, such as transcription from T7 promoter through the origin would proceed in the direction of pAMβ1 replication.

pMTL500E-*ori* corresponds to the construct 2 previously described in Bruand and Ehrlich (26). pMTL500E-*ori*Δ1 and -*ori*Δ2 correspond to pMTL500E-*ori*, except that the 44-bp *ori* sequence has been replaced by deleted forms truncated from the 3′ end: the 36-bp *ori*Δ1 and 27-bp *ori*Δ2, which sequences are shown in Fig. 7*B*.

Purification of the pAMβ1 RepE Protein—The RepE-Intein-CBD fusion protein was cloned under the control of the isopropyl-B-D-thiogalactoside-inducible P_{tac} promoter, and the construct was introduced in *E. coli* cells. Upon isopropyl-B-D-thiogalactoside induction, this RepE-Intein-CBD fusion was overproduced to about 2.5% of total protein and was mainly soluble. Typically, MC1061 cells newly transformed with pCYB*repE* were grown to mid log at 30 °C into 1 liter of LB medium supplemented with 100 μg/ml ampicillin. At A_{650} = 0.6, the culture was shifted to 25 °C, and RepE-Intein-CBD fusion expression was induced by the addition of 1 mM isopropyl-B-D-thiogalactoside for 4 h. All the following operations were carried out at 0 to 4 °C. The cell pellet was resuspended in 25 ml of TENG (20 mM Tris-HCl, pH 8, 0.1 mM EDTA, 1000 mM NaCl, 10% glycerol), sonicated, and centrifuged to yield a clear lysate. The lysate was loaded onto a 5-ml chitin resin column (New England Biolabs), and unbound proteins were washed with 150 ml of TENG in which the NaCl concentration was increased to 2000 mM NaCl. To induce intein-mediated self-cleavage, the immobilized fusion protein was incubated overnight with 100 mM DTT in TENG, resulting in the release of a wild type RepE protein about 80% pure, whereas the intein-CBD fusion remained bound to the column. Ammonium sulfate was added to RepE-containing fractions in TENG to 50% saturation, and the precipitate was dissolved in 1 ml of TENG. The solution was diluted with 20 mM Tris-HCl, pH 8, 0.1 mM EDTA, 10% glycerol to a final concentration corresponding to 200 mM NaCl immediately before loading onto a 1-ml cation exchange Hi-Trap SP column (Amersham Pharmacia Biotech) pre-equilibrated in TENG in which the NaCl concentration was decreased to 200 mM NaCl. The column was washed with the same buffer, and the absorbed proteins were eluted with a step gradient at 640 mM NaCl (in a linear gradient, RepE elutes at about 400 mM NaCl). This step allowed eliminating the main contaminants and the DNA. Ammonium sulfate was added to the pooled fractions to 50% saturation. The precipitate was dissolved in 0.22 ml of TENG and applied at 0.1 ml/min on a 25-ml gel filtration Superdex 75 column (Amersham Pharmacia Biotech) equilibrated in 20 mM Tris-HCl, pH 8, 0.1 mM EDTA, 1000 mM NaCl. This chromatographic step allowed discarding traces of shorter contaminants and of some contaminating fusion protein. For storage, glycerol and NaCl were added to RepE fractions >95% pure to a final concentration of 20% and 1 M, respectively. The protein was then stored in aliquots at −80 °C. No loss of

[2] P. Polard and C. Bruand, personal communication.

activity was observed after at least 1 year. Protein concentrations were quantified using the Coomassie protein assay reagent kit (Pierce) using BSA as a standard. Purity was estimated by SDS-PAGE and SYPRO® red (Molecular Probes) staining (sensitivity similar to that of silver staining).

To avoid aggregation and irreversible inactivation, RepE required throughout the whole purification procedure the presence of 1 M NaCl in Tris-HCl buffer, pH 8, or in phosphate buffers at or above pH 7.5 (insoluble aggregates are formed in phosphate buffers below pH 7.5 and in HEPES or Bicine buffer at pH 8, whatever the salt concentration used). However, temporary dilution at 200 mM NaCl was tolerated. To determine the oligomerization state of RepE, gel filtration chromatography on fast protein liquid chromatography system (Amersham Pharmacia Biotech) was performed as indicated above (in 1 M NaCl), and only one peak corresponding to the monomer was detected. The same chromatographic step performed at 50 mM NaCl allowed us to detect both large aggregates and the monomeric form of RepE.

DNA Substrates for Mobility Shift Assay—The following oligonucleotides were used to make substrates for the binding reaction (uppercase letters indicate sequences from the minimal 44-bp pAMβ1 *ori*; letters in bold in the 61-mer osmg28 series emphasize the sequences that do not pair to the 61-mer osmg27). 75-mer *ori*-W, 5′-gggcgaatcgcgtctgaaAATAAAACCCGCACTATGCCATTACATTTATATCTATGATACGTacgcgaattcgag-3′; 75-mer *ori*-W5′, 5′-gggcgaatcgcgttgtttagctatgatacaggctgaaAATAAAACCCGCACTATGCCATTACAcgcgaattcgag-3′; 75-mer *ori*-W3′, 5′-gggcgaatcgcgtATTTATATCTATGATACGTgtttgttttttctttgctgtttagcgaatgacgcgaattcgag-3′; 56-mer *ori*-W5′, 5′-gggcgaatcgcgtctgaaAATAAAACCCGCACTATGCCATTACAcgcgaattcgag-3′; 45-mer *ori*-W3′, 5′-gggcgaatcgcgtATTTATATCTATGATACGTacgcgaattcgag-3′; 48-mer *ori*-W, 5′-ctgaaAATAAAACCCGCACTATGCCATTACATTTATATCTATGATACG-3′; 75-mer *ori*-C, 75-mer *ori*-C5′, 75-mer *ori*-C3′, 56-mer *ori*-C5′, 45-mer *ori*-C3′, 48-mer *ori*-C, which are reverse complementary to 75-mer *ori*-W, 75-mer *ori*-W5′, 75-mer *ori*-W3′ 56-mer *ori*-W5′, 45-mer *ori*-W3′ and 48-mer *ori*-W, respectively. 61-mer osmg27, 5′- gacgctgccgaattctaccagtgccttgctaggacatctttgcccacctgcaggttcaccc-3′; 61-mer osmg28–21, 5′-gggtgaacctgcaggtgggc**ggctgctcatcgtaggttagt**tggtagaattcggcagcgtc-3′; 61-mer osmg28–15, 5′-gggtgaacctgcaggtgggcaaa**tgctcatcgtaggtt**cactggtagaattcggcagcgtc -3′; 61-mer osmg28–9, 5′-gggtgaacctgcaggtgggcaaagat**tcatcgtag**aggcactggtagaattcggcagcgtc -3′; 45-mer map121, 5′-ctatgagtcgcttttgtaaatttggcaggtactgccatatgctct-3′; 30-mer sda37: 5′-ctaatcaggagaattcgtaatcatggtcat-3′.

For the permutation assay, a set of DNA fragments of similar length (179 to 183 bp) but with the origin located at various positions relative to the fragment ends were isolated from pBend2*ori* either by digestion with different restriction enzymes (filled-in when required by Klenow enzyme) or by PCR using pBend (5′-tcaagaattcacgcg-3′) and *ori*L4 (5′-AATAAAACCCGCACTATGCC-3′) as primers.

The other double-stranded *ori* used were obtained by PCR using either the 75-mer *ori*-W or 75-mer *ori*-C oligonucleotide series as substrates and both 5′-gggcgaatcgcgt-3′ and 5′-ctcgaattcgcgt-3′ as primers or by annealing of the two complementary oligonucleotides. The other non-*ori* dsDNAs used were the 76-bp fragment of pBR322 digested by *Msp*I and filled-in by Klenow enzyme or a 61-bp DNA obtained by annealing of 61-mer osmg27 and its reverse complementary strand. The *n*-nt eye substrates were obtained by annealing the 61-mer osmg27 oligonucleotide with the 61-mer osmg28-*n*. All DNAs used were labeled using either T4 polynucleotide kinase in the presence of [γ-^{32}P]ATP (3000 Ci/mmol) or Klenow enzyme in the presence of [α-^{32}P]dATP (3000 Ci/mmol) and cold dCTP, dGTP, and dTTP, as recommended by the suppliers.

Labeled 75-mer RNA *ori*-W, the perfect RNA counterpart of 75-mer *ori*-W, was obtained from pGEM*ori* linearized by *Eco*RI by *in vitro* transcription from the T7 promoter using [^{32}P]UTP. 75-bp RNA/DNA *ori* was obtained by mixing labeled 75-mer RNA *ori*-W and cold 75-mer *ori*-C in 50 mM NaCl. The mixture was heated for 5 min at 85 °C and allow to cool slowly to room temperature. The complete formation of the RNA/DNA hybrid was verified during the gel retardation experiment, since 75-mer RNA *ori*-W and 75-bp RNA/DNA *ori* clearly have different mobilities.

Mobility Shift Assay—Binding reactions were carried out in 10 μl of 10 mM Tris-HCl, pH 7.5, 70 mM NaCl, 2.5 mM $MgCl_2$, 1 mM DTT, 5% saccharose, 0.005% xylene cyanol, 0.3 mg/ml BSA, 10 μg/ml poly(dI-dC), and 0.1–1 nM labeled DNA substrates unless otherwise specified. Reaction mixtures were incubated at 20–25 °C for 15 min and applied to a running 6% polyacrylamide gel (with either a 1/29 or 1/80 ratio of bisacrylamide/acrylamide) in 25 mM Tris base, 190 mM glycine, 1 mM EDTA. After electrophoresis at 8 V/cm, the gel was dried and exposed to storage phosphor screen. DNA was visualized on a Storm PhosphorImager and quantified using ImageQuant software (Molecular Dynamics). The equilibrium dissociation constants K_d for the RepE-DNA interaction were determined by the method of Carey (37). For this analysis we used a fixed input DNA concentration and various RepE protein concentrations spanning 4 orders of magnitude. Because the DNA concentration in the reaction mixture was much lower than the protein concentration, K_d was approximated as the RepE concentration needed for half-maximal binding of the DNA.

To measure the association rate, complex formation (between 2 nM radiolabeled 75-bp *ori* duplex containing the 44-bp minimal *ori* and 250 nM RepE) was quenched at various times by the addition of 1 μM of unlabeled DNA substrate. For the dissociation rate we let complexes between RepE and labeled 75-bp *ori* form for 10 min, then 1 μM of unlabeled DNA substrate was added, and the amount of complex remaining in the reaction was measured as a function of time.

Preparation of 3′ End Singly Labeled DNA Fragments—To obtain fragments labeled at only one end, pIl253 plasmid DNA was digested with a first restriction enzyme (*Ase*I for the top strand and *Nhe*I for the bottom strand), filled in by the Klenow enzyme (in the presence of [α-^{32}P]dATP (3000 Ci/mmol), [α-^{32}P]dCTP (3000 Ci/mmol), cold dGTP and dTTP), and finally digested with a second restriction enzyme (*Hae*II for the top strand and *Ase*I for the bottom strand). The labeled fragments of interest (220-bp *Ase*I-*Hae*II for the top strand and 167-bp *Nhe*I-*Ase*I for the bottom strand) were then purified using nondenaturing PAGE.

DNaseI Footprinting on 3′ End Singly Labeled DNA Fragments—RepE protein (10–1000 nM) was allowed to bind to its 3′ end singly labeled substrate (0.1–1 nM; ~50,000 cpm) in 50 μl of DNaseI footprint buffer (10 mM Tris-HCl, pH 7.5, 100 mM NaCl, 2.5 mM $MgCl_2$, 1 mM $CaCl_2$, 2 mM DTT, 50 μg/ml BSA, 10 μg/ml poly(dI-dC)) for at least 10 min at room temperature. RepE·DNA complexes were digested with DNaseI (3–6 ng) for exactly 2 min at room temperature, and the digestion was stopped by the addition of EDTA (final concentration of 25 mM). After ethanol precipitation, samples were resuspended in 5 μl of denaturing loading buffer (95% formamide, 20 mM EDTA, 0.05% bromphenol blue, 0.05% xylene cyanol), heated at 80 °C for 5 min before loading on 6% acrylamide-urea sequencing gels, and run in TBE buffer (90 mM Tris borate, 2 mM EDTA, pH 8.3) for 2 h at 60 W. Bands were visualized by direct exposure of the dried gels to storage phosphor screens and analyzed on a Storm (Molecular Dynamics) PhosphorImager.

DNaseI Footprinting on Supercoiled and Linear Plasmid—RepE protein (50–500 nM) was allowed to bind to plasmid pIL253 (0.1–1 μg) either supercoiled or linearized in 50 μl of DNaseI footprint buffer (see above) for at least 10 min at room temperature. RepE·DNA complexes were digested with DNaseI (6–12 ng) for exactly 2 min at room temperature, and the digestion was stopped by the addition of EDTA (final concentration of 25 mM). Cleavage sites were mapped by primer extension as described below.

Orthophenanthroline-Copper (OP-Cu) Footprinting on Supercoiled and Linear Plasmid—RepE protein (50–500 nM) was allowed to bind to plasmid pIL253 (0.1–0.5 μg) either supercoiled or linearized in 20 μl of OP-Cu footprint buffer (10 mM Tris-HCl, pH 7.5, 100 mM NaCl, 2.5 mM $MgCl_2$, 300 μg/ml BSA, 10 μg/ml poly(dI-dC)) for at least 10 min at room temperature. Footprinting reactions were then performed essentially as described by Sigman *et al.* (38). Briefly, reactions were started by adding 2 μl of 1,10-phenanthroline (1 mM), $CuSO_4$ (0.23 mM) and 2 μl of 3-mercaptopropionic acid (58 mM) to the RepE·DNA complexes and incubated for 1 min at room temperature. Digestions were stopped by adding 2 μl of 2,9-dimethyl-1,10-phenanthroline (Neocuproine, 28 mM) and ethanol-precipitated. The four reaction components were from Sigma. Cleavage sites were mapped by primer extension as described below.

Dimethyl Sulfate (DMS) Footprinting on Supercoiled and Linear Plasmid—RepE protein (50–500 nM) was allowed to bind to plasmid pIL253 (0.1–0.2 μg) either supercoiled or linearized in 20 μl of DMS footprint buffer (20 mM Tris-HCl, pH 8, 100 mM NaCl, 2.5 mM $MgCl_2$, 300 μg/ml BSA) for at least 10 min at room temperature. Then, DMS footprinting reactions were performed essentially as described by Sasse-Dwight and Gralla (39). Briefly, reactions were started by adding precisely 0.1 μl of pure DMS (Sigma) for exactly 3 min at room temperature (final concentration 50 mM). Reactions were stopped by adding 40 μl of stop solution (1 M β-mercaptoethanol, 3 M ammonium acetate, 20 mM EDTA), and DMS was carefully eliminated by ethanol precipitation. Methylated nucleotides were mapped by primer extension as described below.

In Vitro $KMnO_4$ Footprinting on Supercoiled and Linear Plasmid—RepE protein (50–500 nM) was allowed to bind to plasmid pIL253 (0.1–1

μg) either supercoiled or linearized in 45 μl of $KMnO_4$ footprint buffer (20 mM Tris-HCl, pH 8, 100 mM NaCl, 2.5 mM $MgCl_2$, 300 μg/ml BSA) for at least 10 min at room temperature. Then, $KMnO_4$ footprinting reactions were performed essentially as described by Sasse-Dwight and Gralla (39). Briefly, reactions were started by adding 5 μl of $KMnO_4$ (50–100 mM) for 2 min at room temperature. Reactions were stopped by adding 50 μl of stop solution (3 M β-mercaptoethanol, 40 mM EDTA, 0.6 M sodium acetate, pH 4.8) and ethanol-precipitated. Modified nucleotides were mapped by primer extension as described below.

In Vivo $KMnO_4$ Footprinting—1A226 (pol^+) or the isogenic *polA5* (pol^-) strain 1A226 carrying either pHV1455 or pHV1455Rep* was grown at 37 °C in MCD medium (K_2HPO_4 62 mM, KH_2PO_4 44 mM, $C_6H_5Na_3O_7$ 3.4 mM, K_2SO_4 11 mM, $MgSO_4$ 0.8 mM, glutamine 0.2%, glucose 0.2%, casamino acid 0.5%, tryptophan 0.01%, histidin 0.005%, phenylalanine 0.005%, and ammonium-iron (III) citrate 11 μg/ml) containing erythromycin 0.6 μg/ml. At A_{650} = 0.5–0.8 and exposed to 10 mM $KMnO_4$ for 2 min essentially as described by Sasse-Dwight and Gralla (39). The reaction was stopped by the addition of 5 mM DTT, the cells were harvested, and plasmid DNA was prepared using either standard alkaline lysis technique or a total DNA extraction procedure (40). Modified nucleotides were mapped by primer extension as described below.

Primer Extension—First, modified plasmids DNAs from DNaseI, OP-Cu, DMS, or $KMnO_4$ footprinting experiments were purified using Qiaquick PCR purification kit spin columns (Qiagen). DNAs were recovered in 30–50 μl of 10 mM Tris-HCl, pH 8.5, and 10–20 μl were used for the primer extension reactions.

Then primer extension reactions were done either using Sequenase or by linear PCR, as described by Sasse-Dwight and Gralla (39). In both cases, primers elc9 (5′-GAGCATACATTCATTCAAGAGAC-3′) and elc17 (5′-CTACTCTCTCCTTCTCCCCC-3′) were used unless otherwise specified. The primers were 5′ end-labeled with [γ-^{32}P]ATP (3000 Ci/mmol) and T4 polynucleotide kinase.

When Sequenase was used, about 150 fmol of supercoiled or linear-modified plasmid (~ 0.5 μg) were denatured with 0.2 M NaOH, neutralized, annealed with 100 fmol of 5′ labeled primer, and incubated for 10 min at 43 °C in 10 μl containing 3 units of Sequenase (Amersham Pharmacia Biotech), 200 μM each dNTP, 20 mM Tris-HCl, pH 7.5, 25 mM NaCl, 10 mM $MgCl_2$, and 10 mM DTT. Reactions were stopped by adding 6 μl of loading buffer (95% formamide, 20 mM EDTA, 0.05% bromphenol blue, 0.05% xylene cyanol).

When linear PCR was used, about 30 fmol of supercoiled or linear modified plasmid (~0.1 μg) were first digested with restriction enzymes to yield fragments ~500 bp long. Samples were then dialyzed on micromembranes (Millipore VS 0.025 μM) for 20 min against Tris-HCl pH8 10 mM and incubated with 100 fmol of 5′-labeled primer in 25 μl containing 1.25 units of *Taq* polymerase (Roche Molecular Biochemicals), 200 μM each dNTP, 10 mM Tris-HCl, pH 8.3, 50 mM KCl, and 2.5 mM $MgCl_2$. Linear amplification was done through 10 cycles of denaturation (94 °C, 30 s), annealing (45 °C, 30 s), and polymerization (72 °C, 30 s). Then 12.5 μl of loading buffer (see above) was added. In both cases (Sequenase or *Taq* polymerase), 8 μl of the mix were heated at 80–90 °C for 5 min before loading on 6% acrylamide-urea sequencing gels and run in TBE buffer (90 mM Tris borate, 2 mM EDTA, pH 8.3) for ~2 h at 60 W.

The regions modified by $KMnO_4$, DNaseI, OP-Cu, or DMS were precisely localized by comparison with dideoxy-sequencing ladders obtained using end-labeled primers on pIL253-unmodified plasmid and run side by side with the footprints. Bands were visualized by direct exposure of the dried gels to storage phosphor screens and analyzed on a Storm PhosphorImager using ImageQuant software (Molecular Dynamics).

RESULTS

Purification of the RepE Protein—Wild type RepE was purified using a C-terminal fusion of the entire protein with a modified intein protein carrying a chitin binding domain (see "Experimental Procedures" and Fig. 1). Purification on a chitin column followed by self-cleavage of the fusion protein resulted in the release of a wild type RepE protein of the expected size (57 kDa). Two further steps of purification led to a protein >95% pure as judged by SDS-PAGE and SYPRO® red staining (Fig. 1*B, lane 5*). Gel filtration chromatography allowed us to determine that RepE is monomeric in solution (data not shown; see "Experimental Procedures").

RepE Specifically Binds to pAMβ1 Double-stranded Origin

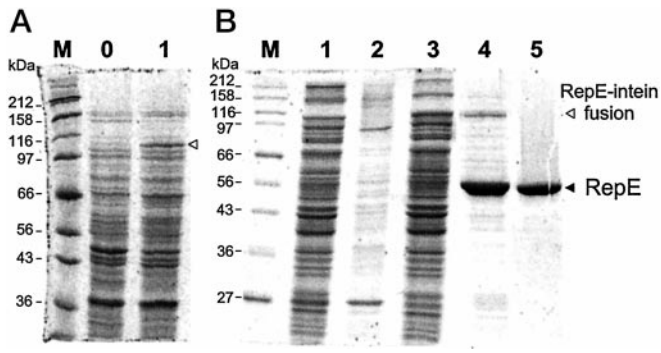

FIG. 1. **Expression and purification of the pAMβ1 RepE protein.** *A*, 20 μg total *E. coli* proteins from cells uninduced (*lane 0*) or induced by isopropyl-B-D-thiogalactoside (*lane 1*) for the expression of the gene encoding the RepE-Intein-CBD fusion were loaded on a 8% SDS-PAGE and stained with SYPRO® red. *B*, protein fractions of the various steps during RepE purification were loaded on a 10% SDS-PAGE: *lane 1*, crude extract from induced cells containing the RepE-Intein-CBD fusion; *lane 2*, insoluble protein fraction; *lane 3*, clarified crude extract; *lane 4*, RepE eluted after DTT-induced self-cleavage; *lane 5*, 2 μg of RepE after gel filtration chromatography; *lane M*, protein size marker. The *black* and *white triangles* indicate the positions of RepE and RepE-Intein-CBD protein fusion, respectively.

Upstream of the Initiation Site of DNA Replication—All known initiator proteins bind to their cognate origin to initiate DNA replication. Despite the absence of known iterons in the minimal 44-bp pAMβ1 origin, we tested whether RepE specifically recognizes and binds *ori*. Binding properties of purified RepE protein were investigated with various *ori* and non-*ori* dsDNA using a gel retardation assay. RepE binds a 75-bp dsDNA carrying the 44-bp minimal *ori* (75-bp *ori*) with a dissociation constant K_d of 18 nM (see Fig. 2*A* and Table I). The DNA sequence recognized by RepE lies in the 5′ end of the minimal *ori* since the K_d of the 56-bp *ori*5′ is in the same range (27 nM) and much lower than that of a 3′ end fragment (>1 μM for the 45-bp *ori*3′). The differences in affinity between the 5′ and 3′ end of *ori* were not due primarily to the different size of the fragments, since similar differences were obtained with the 75-bp *ori*5′ and *ori*3′ (Fig. 2, *B* and *C*, Table I). Finally, RepE does not show any measurable affinity for non-*ori* dsDNA substrates (61- and 76-bp fragments were tested; see Table I and Fig. 3*E*). Therefore RepE binds specifically to the 24-bp part of the origin located 5′ to the initiation site, with an affinity at least 50-fold higher than for non-*ori* dsDNA or the 3′-end of *ori*.

To determine the association and dissociation rates between RepE and the 75-bp *ori*, gel retardation assay was used. Both rate constants could not be determined precisely by this technique, since all complexes were already formed at the shortest time tested (5 s; Fig. 4*A*), and no significant dissociation of the complexes was observed even 30 min after the addition of unlabeled *ori* (Fig. 4*B*). RepE thus recognizes and binds *ori* dsDNA very quickly, the complexes formed being extremely stable.

To confirm and define more precisely the RepE binding site, we carried out DNaseI protection assays on end-labeled pAMβ1 restriction fragments containing minimal *ori* flanked on either side by at least 60 bp of plasmid sequences. A region of 19 nt was protected from DNaseI digestion upon RepE binding on both strands (Fig. 5). The protected areas were situated 5′ to the initiation site, the protected area on the top strand being shifted by 5 nt relative to the protected area on the bottom strand. A site of enhanced sensitivity at a G residue, which reveals a distortion of the double helix, was located in the middle of the protected region on the bottom strand. These results fit the gel retardation data, which define the RepE binding site to a 24-bp region in the 5′ end of the minimal 44-bp

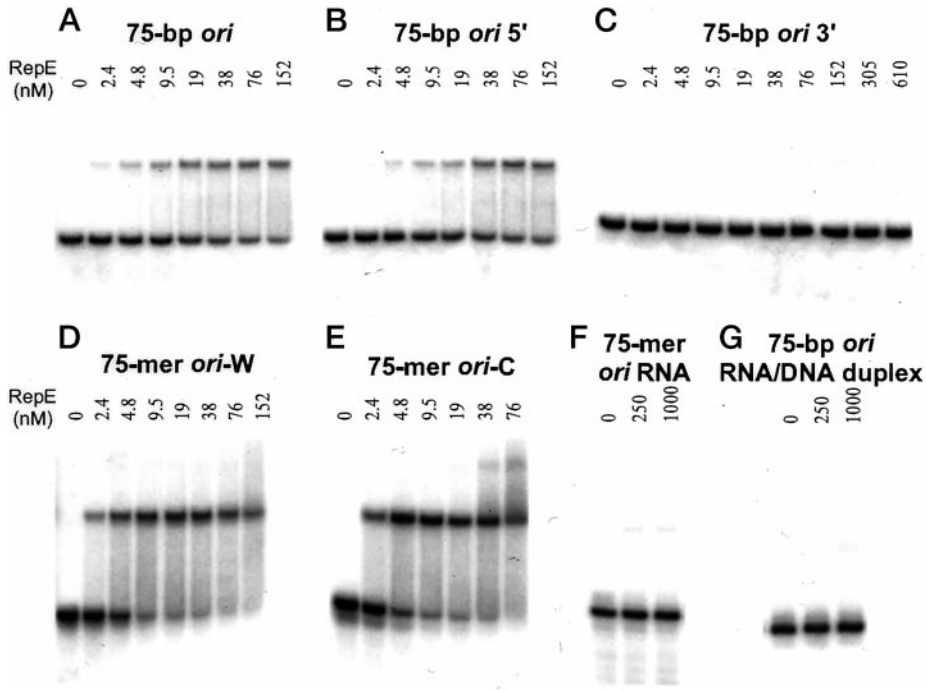

FIG. 2. **Gel retardation analysis of RepE binding to various origin substrates.** Gel retardation assays were carried out in 10 μl as described under "Experimental Procedures" using 0.1–1 nM either dsDNA (*A*, *B*, and *C*), ssDNA (*D* and *E*), RNA corresponding to the transcript through *ori* (top strand; *F*) or RNA/DNA *ori* duplex (*G*), 100 ng of poly(dI-dC), and the indicated concentrations of RepE protein. Scheme and nucleotide sequences of the substrates are presented in Table I and under "Experimental Procedures," respectively.

ori. The K_d estimated from the DNaseI protection assays was in the same range as that measured by gel retardation assays (15–30 nM).

RepE Binds with High Affinity to ssDNA and Does Not Bind to RNA-containing Substrates—A prerequisite for initiation of DNA synthesis is the opening of the origin, which results in the appearance of ssDNA. We therefore tested the affinity of RepE for ssDNA in a gel retardation assay using various *ori* and non-*ori* oligonucleotides (Fig. 2 and 3 and Table I). RepE bound to ssDNA containing a complete *ori* (75-mer *ori*-W and *ori*-C) with an affinity about 5-fold higher than comparable dsDNA (Fig. 2, compare *panels A*, *D*, and *E*). This affinity decreased only slightly (2-fold) when either truncated origins or non-origin ssDNAs were used, provided that their size was longer than about 60 nt (see Table I). The affinity decreased greatly for shorter segments, the DNA/RepE interaction being too weak to withstand electrophoretic analysis, which led to a smear of the DNA during the gel-shift assay (data not shown). As observed for the dsDNA *ori* substrate, the association of RepE to 75-mer ssDNA *ori* was very quick ($k_{ass} < 5$ s), and the complexes formed were extremely stable ($k_{diss} \gg 30$ min; data not shown).

Opening of the origin should lead to the formation of a ssDNA bubble within a dsDNA region. We therefore tested RepE affinity for such structures in a gel retardation assay using segments of 61 bp with central bubbles of 9, 15, or 21 nt. A very high affinity similar to that obtained with the 75-mer ssDNA *ori* was found with the 21-mer bubble (K_d = 5 nM, Fig. 3*B*). Furthermore, a second retarded complex as well as traces of other uncharacterized complexes that may reflect the binding of additional Rep molecules appeared at higher RepE concentrations. The affinity of RepE for bubble substrates decreased about 2.5- and 40-fold when the size of the bubble decreased to 15 and 9 nt, respectively (Fig. 3, *C* and *D*). We conclude from these results that RepE has a high affinity for bubble structures provided that the ssDNA region is at least 15 nt long.

Initiation of pAMβ1 replication requires transcription of the origin. We therefore investigated RepE binding to different *ori* ribonucleotide substrates. A 75-mer transcript corresponding to the leading strand of the origin and, thus, mimicking a putative initiator transcript, was synthesized *in vitro*, and its affinity for RepE was tested either in the RNA form (75-mer RNA *ori*-W) or as RNA/DNA duplex (75-bp RNA/DNA *ori*). We did not detect a measurable affinity between RepE and the RNA-containing substrates (Fig. 2, *F–G*, Table I).

RepE Binding Moderately Bends the Double-stranded Origin Upstream of the Initiation Site—Sequence-specific DNA-binding proteins frequently contort DNA by bending at the site of interaction (41). In the case of replication origin-binding proteins, this bending may facilitate open complex formation. To test whether RepE bends the double-stranded origin, we employed the gel retardation analysis of permuted fragments (42). A set of fragments of identical size, with the origin at variable positions relative to the fragment ends, was generated from plasmid pBend2*ori*, which contains the 44-bp minimal *ori* inserted between two tandemly repeated multicloning sites. As seen by gel retardation, free DNA *ori* segments migrate homogeneously, indicating that they do not possess any natural bend, whereas the complexed fragments show a characteristic bell-shaped curve (Fig. 6). This demonstrates that binding of RepE to the origin introduces a curvature in the DNA. However, the bending angle was very modest, only 31.3° (±0.6°, four independent experiments). The bent zone, identified as the center of the most retarded segments, is located just upstream from the initiation site of DNA replication in the region protected against DNaseI action upon RepE binding.

RepE Distorts the AT-rich Sequences Downstream from the Initiation Site in Vivo and in Vitro—To test whether RepE destabilizes the DNA pairing at the origin, potassium permanganate ($KMnO_4$) footprinting was used. This drug oxidizes thymines (and to a lesser extent cytosines) at unwound or sharply distorted DNA sites (43–45). The modified nucleotides are easily detected on supercoiled DNA by primer extension, since DNA polymerases are unable to copy oxidized residues (46). Since $KMnO_4$ efficiently enters bacterial cells, it can be used conveniently for both *in vivo* and *in vitro* distortion mapping (39).

In vivo, $KMnO_4$ footprints were carried out using *B. subtilis* cells harboring plasmid pHV1455, a hybrid of a functional pAMβ1 replicon (pIL253) and a pTB19 replicon. Exponentially growing cells were submitted to $KMnO_4$ treatment as described

TABLE I

Equilibrium dissociation constants (K_d) of RepE on various nucleic acid substrates

The affinity of RepE for various nucleic acids was determined using gel retardation assays as described under "Experimental Procedures." A scheme of the various *ori* nucleic acids used is given indicating the initiation site of the leading strand (bent arrow), the parts of the minimal *ori* located either 5′ (24-nt long, gray rectangle), or 3′ (20-nt long, hatched rectangle) from the initiation site, the non-specific DNA from the top strand (-W, black line) or the bottom strand (-C, dotted line), and non-specific RNA from the top strand (broken line). The drawings are made on scale.

Nucleic acid substrate	Scheme	K_d (nM)
	← 44-bp minimal *ori* →	
ori dsDNA		
75-bp *ori*		18 ± 5
56-bp *ori5'*		27 ± 3
75-bp *ori5'*		15 ± 2
45-bp *ori3'*		>1000
75-bp *ori3'*	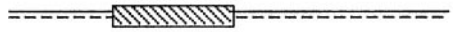	>1000
non-ori dsDNA		
76-bp pBR322		>1000
61-bp osmg27		>1000
ori ssDNA		
75-mer *ori*-W		4 ± 1
75-mer *ori*-C		6 ± 2
75-mer partial origins [1]		11 ± 4 [1]
non-ori ssDNA		
61-mer osmg27 or 28		13 ± 4
45-mer map121		~300 [2]
30-mer sda37		~600 [2]
RNA & RNA/DNA duplex		
75-mer RNA *ori*-W		>1000
75-bp RNA/DNA *ori*	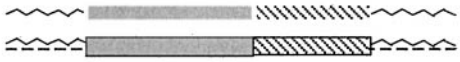	>1000

[1] 8 different 75-nt-long ssDNA substrates carrying partial sequences of the origin and either strand were tested for RepE binding and showed similar affinity.

[2] ~ indicates that upon the conditions used (migration at room temperature), RepE/DNA interactions were unstable. The complexes dissociate during electrophoresis, which resulted in a smear of labeled DNA migrating between the free material and the most retarded one. K_d were estimated considering the smear as part of the shifted material.

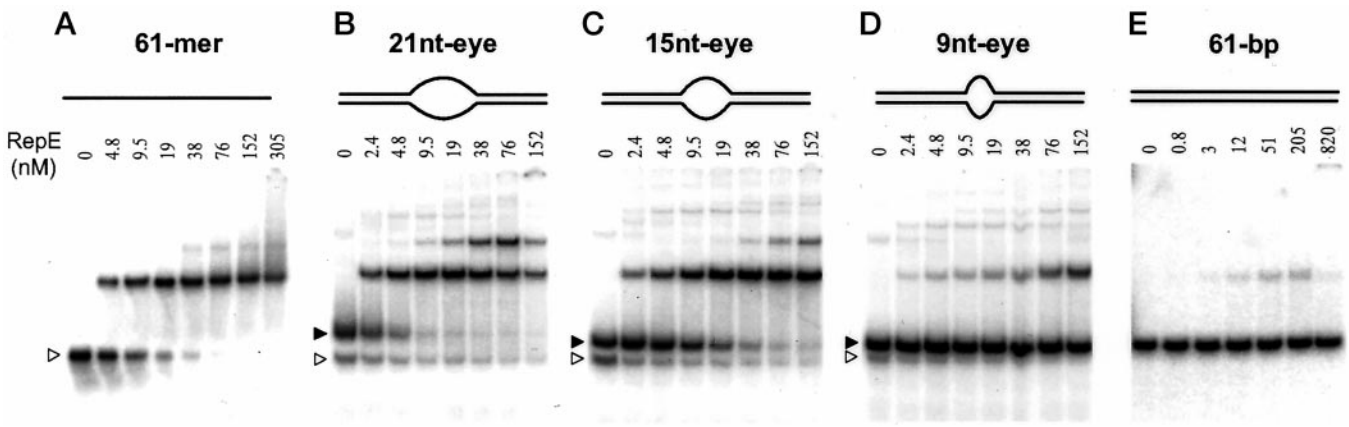

FIG. 3. **Gel retardation analysis of RepE binding to various non-origin substrates.** Gel retardation assays were carried out as described under "Experimental Procedures" and in the legend of Fig. 2. Non-origin substrates of 61 nucleotides were used, present either in a single-stranded (*A*) or double-stranded (*E*) form or as partial double-stranded substrates with a central single-stranded bubble of 21, 15, and 9 nt (*B*, *C*, and *D*). All substrates were made using the labeled 61-mer osmg27 oligonucleotide alone (*A*) or annealed with fully (*E*) or partially (*B–D*) complementary oligonucleotides. The *white* and *black triangles* indicate the migration position of the 61-mer and the various bubbles in the free form, respectively.

under "Experimental Procedures." Little modification of *ori* top strand was observed *in vivo* when *repE* was inactivated by a frameshift mutation (Fig. 7, *A*, *RepE* −). In the presence of RepE, specific sites were hyper-reactive, covering about 20 nt on the top strand, immediately downstream from RepE binding site. The reactivity was independent from DNA synthesis, since

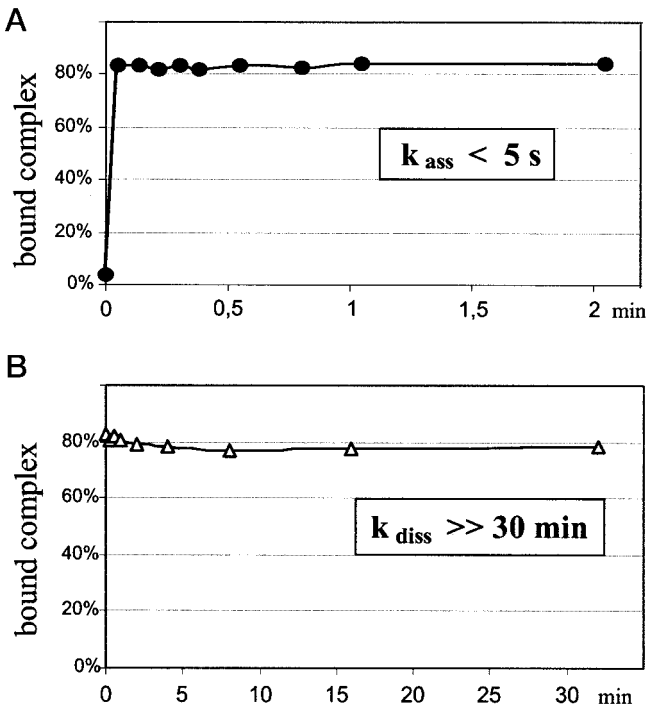

FIG. 4. **Association and dissociation rates of 75-bp *ori*·RepE complexes.** Complex formation between 2 nM radiolabeled 75-bp *ori* duplex containing the 44-bp minimal *ori* and 250 nM RepE was quenched at various time with a 500-fold excess of unlabeled 75-mer *ori*-W either immediately (association rate) or 10 min after RepE addition (to let the complex reach an equilibrium; dissociation rate). The ratio of dsDNA *ori* bound to RepE at different times was quantified after gel electrophoresis using a Storm PhosphorImager. The data were used to plot the time courses for association (*A*) and dissociation (*B*) between RepE and 75-bp *ori*.

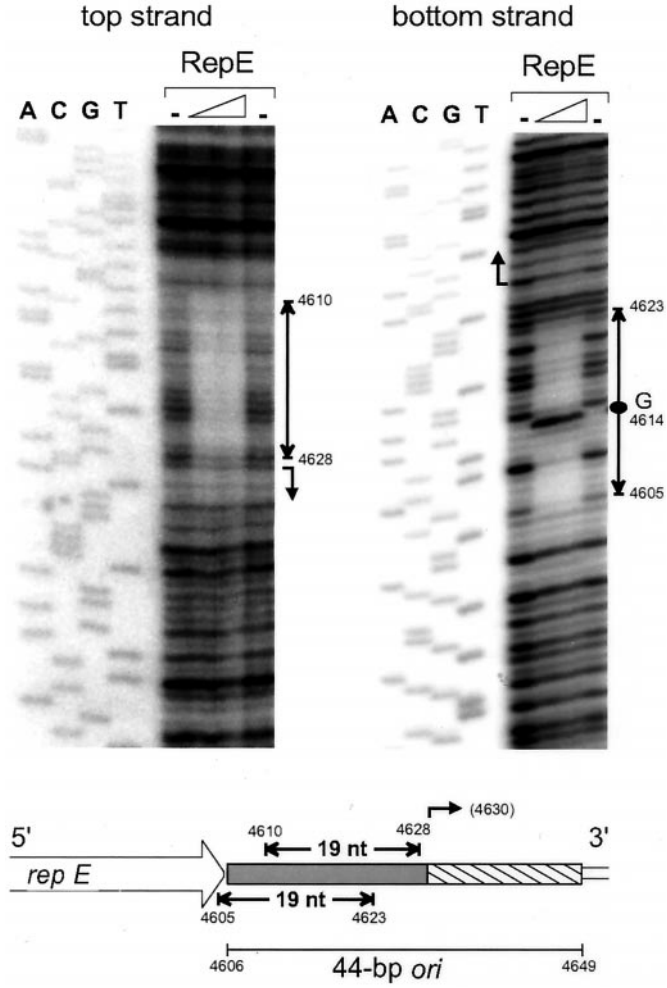

FIG. 5. **DNaseI footprint of RepE bound on *ori* fragments.** *Top*, sequencing gel displaying DNaseI protection pattern of each *ori* strand in the absence and in the presence of RepE. *ori*-containing pAMβ1 restriction fragments were labeled at one end of the top (*left panel*) or the bottom strand (*right panel*) and incubated with 0, 200, and 800 nM RepE. Treatment with DNaseI and subsequent separation through a 6% polyacrylamide-urea denaturing gel were as described under "Experimental Procedures." The region protected from cleavage is indicated by *double-headed arrows*, and the initiation site of the leading strand synthesis is represented by a *bent arrow*. The *black oval* indicates a site of increased sensitivity on the bottom strand at a G residue. *Numbers* refer to the nucleotide sequence of pAMβ1 (GenBank™ access number AF007787). *Lanes ACGT* correspond to a ladder of M13mp18 dideoxy sequence with M13/pUC sequencing primer −40. This control sequence allowed determination of the size of the protected DNA fragments and the position of the footprints relative to the *ori* sequence. *Bottom*, schematic representation of the *ori* region with the DNaseI footprints of RepE data relative to the initiation site (*bent arrow*), the *repE* gene (*open boxed arrow*), and the 5′ and 3′ parts of the minimal 44-bp *ori* (*gray* and *hatched boxes*, respectively).

similar patterns were obtained in *polA*$^-$ and *polA*$^+$ contexts. The band of strong intensity at the initiation site, detected in the *polA*$^+$ context but not in the *polA*$^-$ context, originated from primer extension occurring on the newly synthesized leading strand extruded during DNA preparation from D-loop replication intermediates. RepE-dependent and Pol I-independent modifications of the bottom strand were also observed, but in a much narrower region (4–7 nt), encompassing the initiation site (Fig. 7*A*). We conclude that RepE-dependent distortion of the AT-rich region of the origin is revealed by $KMnO_4$ oxidation *in vivo*.

To gain further insight into the distortion mechanism and analyze the parameters involved in this process, we performed *in vitro* $KMnO_4$ footprints. The role of RepE was investigated using pIL253, either in a supercoiled or linear form. This plasmid was incubated with or without purified RepE and submitted to $KMnO_4$ treatment. Specific sites became hyper-reactive to $KMnO_4$ oxidation upon RepE addition when supercoiled DNA was used. These sites are grouped in a ~23-bp region covering both DNA strands, immediately downstream from RepE binding site (Fig. 7*A*). This region did not show any peculiar reactivity toward $KMnO_4$ in the absence of RepE, indicating that it does not behave as a DNA-unwinding element. The reactivity required a negatively supercoiled DNA substrate, since plasmid linearization rendered the origin completely resistant to $KMnO_4$ oxidation. Thus, distortion of the origin requires RepE as the sole protein factor and depends strictly on DNA supercoiling. Interestingly, the oxidation patterns obtained *in vivo* and *in vitro* were highly similar for the top strand, suggesting that RepE alone promotes denaturation of the origin *in vivo*. In contrast, clearly different patterns were obtained for the bottom strand (see "Discussion").

The relative importance of *ori* and flanking sequences for $KMnO_4$ sensitivity was investigated using pAMβ1 derivatives carrying either the entire 44-bp minimal *ori* cloned into a different locus or truncated origins. The extent of the deletions is shown Fig. 7*B* (*bottom*; these plasmids, pMTL500E-*ori*, -*ori*Δ1, and -*ori*Δ2, replicate in *E. coli* by their pUC moiety). Whereas pMTL500E-*ori* efficiently transformed *B. subtilis* cells and was maintained at a high copy number, the deletion of the 3′ end of the origin completely abolished the transformation ability of the pMTL500E-*ori*Δ plasmids (data not shown). Supercoiled forms of the three plasmids were submitted to $KMnO_4$ oxidation *in vitro*. The $KMnO_4$ modification pattern of the minimal origin at this new locus was identical to that obtained with pIL253, which showed that the helix distortion of

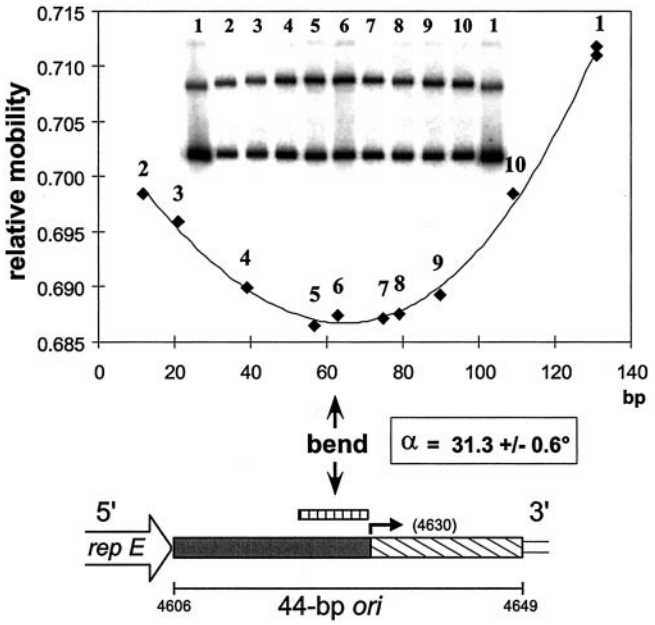

FIG. 6. **Gel retardation analysis of permuted fragments containing the minimal origin.** *Inset*, gel retardation assay carried out as described under "Experimental Procedures" using a set of DNA fragments of similar length (179 to 183 bp) but with the origin located at various positions relative to the fragment ends followed by separation through 6% polyacrylamide gel. The fragments used were generated from pBend2*ori* either by PCR using as primers pBend and *ori*L4 (*lane 1*) or by restriction with the enzymes *Bgl*II (*lane 2*), *Sfa*NI (*lane 3*), *Xho*I (*lane 4*), *Dra*I (*lane 5*), *Pvu*II (*lane 6*), *Sma*I (*lane 7*), *Ssp*I (*lane 8*), *Tfi*I (*lane 9*), or *Bam*HI (*lane 10*). *Graph*: for each *lane*, the relative mobility μ of DNA was calculated (μ = mobility of the retarded DNA/mobility of free DNA) and plotted against the position of the binding site. The result obtained with one out of the four independent experiments carried out is shown. The bending angle α, obtained by using the empirical formula $\cos \alpha/2 = \mu_{min}/\mu_{max}$ (73), is indicated. *Bottom*, the minimal 44-bp *ori* is schematized as in Fig. 5. The position of the maximum of bending induced by RepE is indicated by a *hatched rectangle*.

the origin is independent from flanking sequences (Fig. 7*B*, *top*). In contrast, the pattern of the truncated origins was highly affected; it showed a shorter modification zone, restricted to the remaining *ori* sequences (17 nt for the *ori*Δ1 derivative; about 10 nt for *ori*Δ2). Because the distorted region of the full-length 44-bp *ori* is particularly AT-rich (85% for the 23-bp distorted region *versus* 68% for the whole origin), the disappearance of $KMnO_4$ modification observed with *ori* Δ1 and Δ2 may be explained by the replacement of this AT-rich region by a more GC-rich region (Fig. 7*B*, *bottom*). These results suggest that the RepE-mediated distortion of the complete AT-rich region of the origin is essential for initiation of DNA replication.

RepE Melts the AT-rich Sequence of the Origin, Forming an Open Complex in Vitro—$KMnO_4$ reacts not only with fully melted DNA, but also with bent, unstacked, or untwisted DNA (45, 47). Both the size of the modified region and the fact that pyrimidine residues on both strands were reactive with $KMnO_4$ *in vitro* argue in favor of melted rather than only distorted DNA in pAMβ1. To confirm this conclusion, we used a DMS footprint technique (39). DMS modifies differently dsDNA and ssDNA. On dsDNA substrates, it methylates mainly the N-7 of guanines (48), whereas on ssDNA, it modifies N-1 of adenine and, to a lesser extent, the N-3 of cytosine (49). pIL253-supercoiled DNA, complexed or not with RepE, was treated with DMS, and modified residues were mapped by primer extension using *Taq* polymerase. The main signals obtained with dsDNA substrates in the absence of RepE corresponded to guanines presumably methylated at N-7 (Fig. 8). In the presence of RepE, new signals corresponded mainly to A and C residues in the distorted region revealed by the $KMnO_4$ technique and on both strands (a weak protection of RepE binding site is also detected; see next paragraph). Their appearance argues that the distorted region corresponds to a truly melted region. However, the signals were faint and strictly dependent on the concentrations of DMS and RepE. This can be due either to the fact that not all molecules were denatured or to incomplete accessibility of DMS to the ssDNA. Moreover, we were unable to detect ssDNA in this AT-rich region of the origin by nuclease P1 cleavage in the presence of RepE (data not shown). These results suggest that an open complex is formed at the origin, but intense DMS modification and enzymatic attack of the ssDNA are prevented, possibly by further binding of RepE on this region (see "Discussion").

In addition to the enhanced signals detected in the AT-rich region, a very faint protection (~40% in the top strand and ~40–60% in the bottom strand) was obtained in the region of the RepE double-stranded binding site (Fig. 8). The reason for this weak footprint cannot be due to a poorly active protein, since another footprinting reagent used in the same experiment, the chemical nuclease OP-Cu (see "Discussion"), revealed a clear protection of the RepE binding site. It is possible that the ineffective protection against DMS might be due to the fact that this reagent acts at the major groove of DNA. This may thus be indicative of a binding of RepE in the minor groove of dsDNA (see "Discussion").

Additional RepE Binding to the Melted Region of the Open Complex in Vitro—Our results suggest that RepE is able to denature ~25 nt in the 3′ end of the origin on supercoiled molecules and show that it binds efficiently to oligonucleotides forming bubble structures with ssDNA regions of at least 15 nt. Thus, we wondered whether additional RepE molecules could bind to the melted region of the open complex. To test this hypothesis, DNaseI and the chemical nuclease OP-Cu were used as footprinting reagents of RepE·*ori* complexes formed on supercoiled DNA, searching for an extension of the footprint observed on linear dsDNA. Neither reagent has any sequence specificity, and they both cleave the DNA through its minor groove. Mapping of the cleaved residues was done by primer extension on supercoiled pIL253 plasmids. As expected, an extended protection pattern, covering both RepE double-stranded binding site and about 30 nt downstream on both strands was clearly observed using OP-Cu footprints (Fig. 9). A similar extended protection area was also observed with DNaseI, although it was much fainter in this case (data not shown, but the result is summarized in Fig. 10). These results show that on supercoiled substrates RepE binding on dsDNA renders the downstream AT-region reactive for fixation of extra RepE molecules. Additionally, the clear footprint of the double-stranded binding site of RepE obtained with DNaseI and OP-Cu, in contrast to the weak one obtained with DMS, supports the hypothesis that RepE binds the DNA in the minor groove.

DISCUSSION

The initiation mechanism of pAMβ1 replication is original because it requires a small unstructured origin, an initiator protein (RepE), a transcription fork passing through the origin codirectional to DNA synthesis and Pol I but not DnaA. To better understand this process, we have characterized the RepE/*ori* interaction. Our observations show that RepE possesses some of the features expected for an initiator together with some unexpected properties. Indeed, RepE binds, bends, and melts the origin in a supercoiling-dependent way to form an open complex. However, the double-stranded origin contains a single RepE binding site (there is no iterons), the bend is

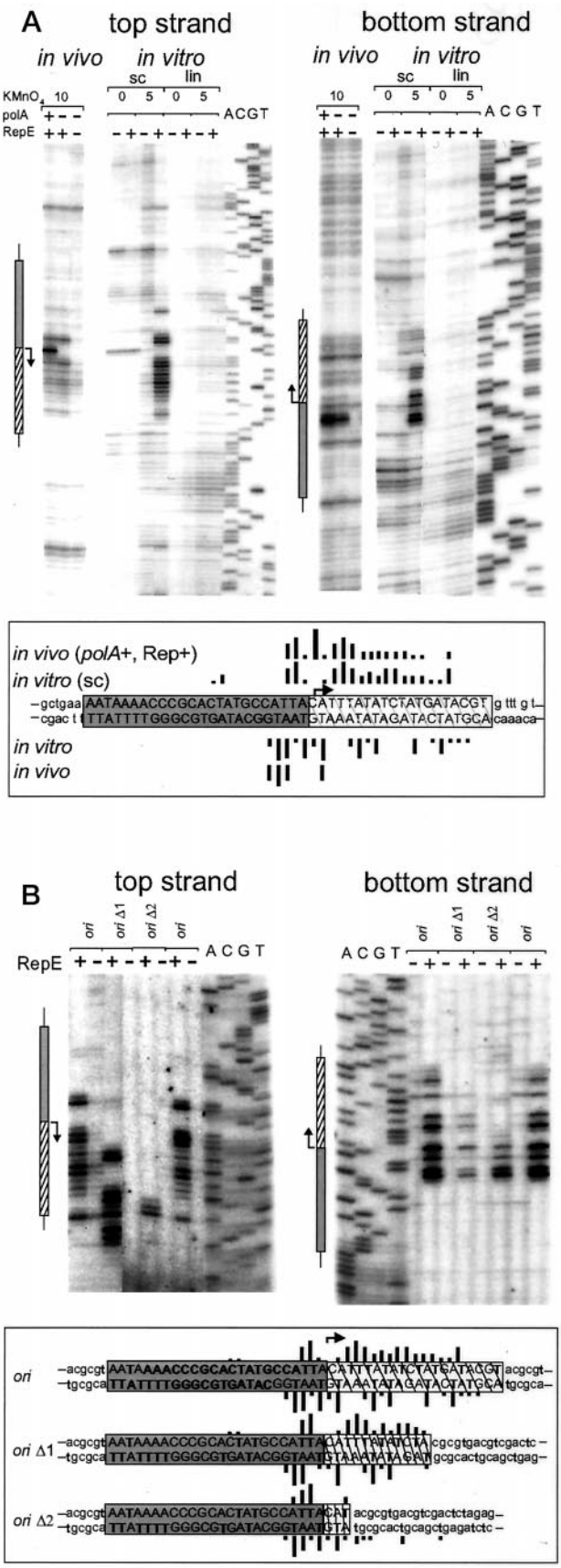

FIG. 7. ***In vivo* and *in vitro* $KMnO_4$ sensitivity of pAMβ1 *ori*.** *A*, $KMnO_4$ oxidation patterns of pAMβ1 derivatives *in vivo* and *in vitro*. *In vivo*, exponentially growing *B. subtilis* cells of either wild type (*polA*+) or deficient in Pol I (*polA*5) carrying plasmid pHV1455 or a derivative inactivated for RepE synthesis (pHV1455*) were submitted to 10 mM $KMnO_4$ treatment for 2 min as described under "Experimental Procedures." *In vitro*, 1 μg of pIL253 plasmid either supercoiled (*sc*) or linear (*lin*) was incubated 10 min at room temperature with or without (+ or −) 120 nM RepE and treated with $KMnO_4$ (0 and 5 mM). Modification of the top and bottom strands were mapped by primer extension, using labeled primers elc17 and elc9, respectively. The same primers and unmodified pIL253 DNA were used for the control sequencing ladders (*lanes ACGT*). A schematic representation of the minimal 44-bp *ori* is positioned on the left of each *panel* (schematized as in Fig. 5). At the bottom of the *panel*, a comparison of the $KMnO_4$ modifications obtained *in vivo* and *in vitro* is represented. The sequence in *boxed uppercase letters* corresponds to the minimal 44-bp *ori*. The *black bars* above and below the sequence indicate the location and intensity of the modifications induced by $KMnO_4$ on the top and bottom strands, respectively. *B*, $KMnO_4$ oxidation patterns of truncated *ori*. Supercoiled plasmids with either the wild type minimal 44-bp *ori* (pMTL500E-*ori*) or truncated forms containing the RepE binding site but lacking part of the sequences located downstream from the initiation site (pMTL500E-*ori*Δ1 and -*ori*Δ2) were treated as described above (except that a $KMnO_4$ concentration of 5 mM was used). The primer extensions were done using the M13/pUC reverse sequencing primer −24 (top strand) and the sequencing primer −40 (bottom strand). On the left of each *panel*, only the wild type *ori* is schematized. At the bottom of the figure, a comparison of the $KMnO_4$ modifications obtained for the wild type and the truncated origins is given schematically. The legend is as for *panel A*.

weak, and RepE binds nonspecific ssDNA more efficiently than dsDNA. Very importantly, the melted DNA in the open structure is a substrate for further RepE binding. We thus speculate that in open complex formation, the ssDNA binding activity compensates for the weak bend and for the lack of RepE oligomerization on the double-stranded origin.

RepE Interaction with the Double-stranded Origin—Using gel retardation assays and *in vitro* footprint experiments, specific and efficient binding was observed between RepE and the double-stranded origin (K_d ~ 20 nM). The binding site was mapped to the 25-bp sequence located upstream from the initiation site. Careful examination of this sequence did not reveal any repeated sequence longer than 2 bp, which suggests that pAMβ1 differs from the previously described initiator-encoding replicons by having a unique binding site for the initiator protein in the double-stranded origin (see Ref. 8 for review). Even replicons such as R1, reported as lacking iterons, possess more than one binding site (with a 5-bp common core sequence) for the initiator protein (50). Thus, whatever the replicon, multimers of the initiator protein are involved in origin binding and initiation of replication. In contrast, a single RepE molecule appears to bind to the pAMβ1 double-stranded origin since (i) a unique complex is detected by gel shift analysis, and (ii) RepE is a monomer in solution. However, when the plasmid is supercoiled, several monomers of RepE bind to the origin as discussed below.

Comparison of the footprints obtained at RepE double-stranded binding site with various reagents (DNaseI, OP-Cu, DMS) reveals some interesting features (see Fig. 10 for a summary). Efficient protection (70–95%) against reagents that act in the minor groove of the DNA (DNaseI or OP-Cu) was observed, whereas the protection against reagents that act in the major groove (DMS) was much weaker (40–60%). Taken together, these results suggest that RepE binds primarily in the minor groove of the 5′ end of the origin. Binding in the minor groove has been demonstrated for protein p6 from *B. subtilis* phage Φ29 (a nonspecific dsDNA-binding protein that activates the initiation of Φ29 DNA replication (51)) and for many architectural factors that introduce large bends in the DNA (such as the prokaryotic IHF and HU proteins and the eukaryotic HMG proteins (52, 53)). However, the initiators DnaA from *E. coli* and RepA from pPS10 were shown to interact with both major and minor grooves (54, 55).

Open Complex Formation and Binding of Additional RepE on the Melted DNA—A number of studies in prokaryotic and

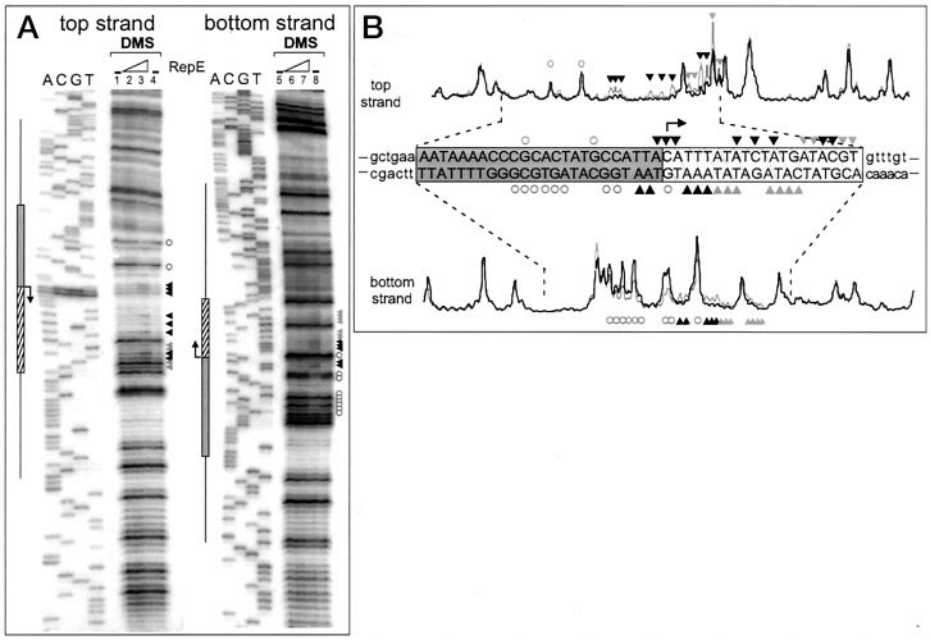

FIG. 8. **DMS footprint of RepE bound on supercoiled substrates.** *A*, sequencing gel displaying DMS sensitivity of each strand around *ori* in the absence and in the presence of RepE. Supercoiled pIL253 DNA was incubated without *(lanes 1*, *4*, *5*, and *8)* or with 300 nM *(lanes 2* and *6)* and 500 nM *(lanes 3* and *7)* RepE for 10 min at room temperature and treated with DMS as described under "Experimental Procedures." The modification sites on the top *(lanes 1–4)* and bottom *(lanes 5–8)* strands were mapped by primer extension using labeled primers elc17 and elc9 respectively followed by separation through a 6% polyacrylamide-urea sequencing gel. The same primers were used for the control sequencing ladder (*lanes ACGT*). A schematic representation (as in Fig. 5) of the minimal 44-bp *ori* is positioned on the left of each *panel*. Nucleotides partially protected by RepE against DMS modification are indicated with *gray open circles*. Nucleotides showing marked and slightly increased DMS sensitivity upon RepE binding are indicated with *black* and *gray triangles*, respectively. *B*, quantification of the experiment shown in *A* by Storm PhosphorImager analysis using ImageQuant software. Scans of *lanes 3–4* (*top strand*) and 7–8 (*bottom strand*) are drawn at the top and the bottom of the *panel*, respectively. To facilitate the comparison, the scans obtained for each strand with naked DNA (*black line*) and RepE-bound DNA (*gray line*) are superimposed. A schematization of the *ori* region is presented with the same symbols as defined above.

eukaryotic genomes sustain the idea that the origin must be strongly bent for duplex opening, allowing subsequent entry of the replicative helicase (4, 56, 57). Sharp bending of the origin occurs consequent to the binding of multimers of the initiator (58–60) and may be helped by an intrinsic curve in the DNA (61, 62). Unlike these replicons, pAMβ1 origin does not possess any intrinsic bending and only a very weak bend (31°) is induced by RepE binding on linear fragments containing the origin (Fig. 6). This raises the question about the existence of other factors that could enhance this bend and about its function in pAMβ1 initiation. Several convergent data suggest that, on supercoiled substrates, RepE binding promotes the denaturation of the downstream AT-rich region. *In vitro*, $KMnO_4$ footprints show that RepE binding highly distorts the AT-rich region of the origin (Fig. 10). This distortion is strictly dependent on RepE, the presence of the AT-rich sequence, and the supercoiling of the *ori*-containing substrates. DMS footprint experiments revealed a significant increase in the methylation of the A and C residues of the AT-rich region upon RepE binding at the origin (Fig. 10). This indicates that the AT-rich region is melted. Interestingly, DNaseI and OP-Cu footprints performed on supercoiled templates revealed protections extending from the RepE binding site to more than 30 nt downstream, covering the AT-rich region. These extended footprints together with the fact that RepE binds with a high affinity to dsDNA fragments containing single-stranded bubbles at least 15 nt-long (Fig. 3) suggest that RepE binds the melted region of the origin, protecting it from DNaseI or OP-Cu cleavage. RepE binding in the melted region could explain both the weak accessibility of DMS to the ssDNA and the lack of P1 sensitivity on supercoiled *ori*-containing plasmid in the presence of RepE. Such a resistance of an origin melted region to P1 nuclease has been described in other systems such as simian virus 40 (47). The fact that the extended footprints observed either with OP-Cu or DNaseI did not reveal 100% protection upon RepE binding might be explain by several hypotheses. First, RepE might not bind to all the supercoiled molecules. Second, some cleavage of ssDNA might occur even in the presence of RepE. Third, binding of RepE might be dynamic, leading to sliding of the protein along ssDNA. Finally, although RepE dissociates from ssDNA very slowly, re-annealing of the melted region could displace the protein from its ssDNA-binding site.

Possible Role for the Strong ssDNA Binding Activity of RepE—As shown by gel retardation assays, RepE does not bind nonspecific dsDNA but binds efficiently *ori*-containing dsDNA and even more efficiently any ssDNA. Other initiators have been found to possess some ssDNA binding activity. Preferential binding of DnaA to the upper strand of the open complex at *oriC* was suggested because of the poor cleavage of this strand by P1 nuclease compared with that of the lower strand (4). However, although bacteriophage λ O initiator protein has been shown to bind short (43 nt) oligonucleotides (although weakly and nonspecifically (63)), no oligonucleotide binding was detected for DnaA protein in the same system or in others (54). Intrinsic but low and nonspecific ssDNA binding activities have been described for simian virus 40 T-antigen (64) and minute virus of mice NS1 (65), which are helicases and, thus, require for this function some affinity for ssDNA. An exception among initiators, for which an affinity similar for *ori*-containing dsDNA and nonspecific ssDNA has been described, is the origin recognition complex (ORC) from *Saccharomyces cerevisiae* (66). Similar to what we found for RepE, the strength of the ORC-ssDNA interaction is correlated to the ssDNA length. Binding of ORC to ssDNA alters ORC conformation and stimulates ORC ATPase, thus regulating ORC function and initiation of replication (ORC-ADP is inactive for binding to the

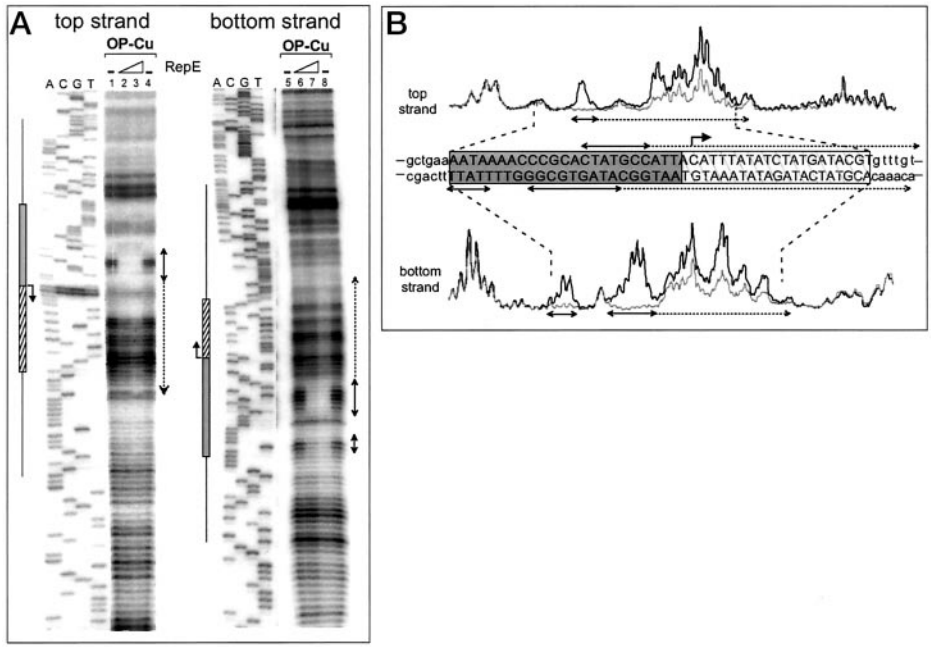

FIG. 9. **OP-Cu footprint of RepE bound on supercoiled substrates.** *A*, sequencing gel displaying OP-Cu protection pattern of each strand around *ori* in the absence and in the presence of RepE. Supercoiled pIL253 DNA was incubated without *(lanes 1*, *4*, *5*, and *8)* or with 300 *(lanes 2* and *6)* and 500 nM *(lanes 3* and *7)* RepE for 10 min at room temperature and treated with OP-Cu as described under "Experimental Procedures." The cleavage sites on the top and bottom strands were mapped by primer extension using labeled primers elc17 and elc9, respectively, followed by separation through a 6% polyacrylamide-urea sequencing gel. The same primers were used for the control sequencing ladder (*lanes ACGT*). A schematic representation (as in Fig. 5) of the minimal 44-bp *ori* is positioned on the left of each *panel*. Protected regions are represented as *double-headed arrows*; *solid lines* indicate the regions strongly (>40%) protected from OP-Cu modification, whereas *dashed lines* indicate extended and weaker footprints observed only on supercoiled DNA at the highest RepE concentration used. *B*, quantification of the experiment shown in *A* by Storm PhosphorImager analysis using ImageQuant software. Scans of *lanes 3–4* (*top strand*) and *7–8* (*bottom strand*) are drawn at the top and the bottom of the *panel*, respectively. To facilitate the comparison, the scans obtained for each strand with naked DNA (*black line*) and RepE-bound DNA (*gray line*) are superimposed. A schematization of the *ori* region is presented with the same symbols as defined above.

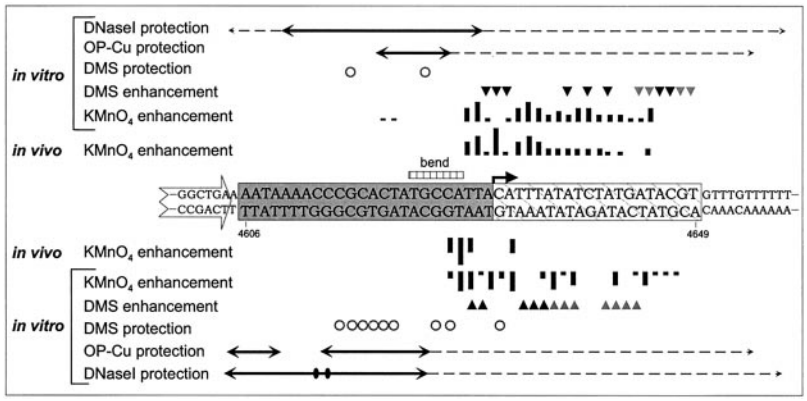

FIG. 10. **Summary and schematic representation of the RepE footprints on the *ori* region.** A compilation of DNaseI, OP-Cu, $KMnO_4$, and DMS footprinting data, collected from the experiments shown in Figs. 5–9, is presented. The 44-bp minimal *ori* sequence is *boxed* and represented with its 5′ part from the initiation site (*bent black arrow*) as *uppercase letters on a gray background*, and its 3′ part is represented as *uppercase letters on a hatched background*. *Numbers* refer to the nucleotide sequence of pAMβ1 (GenBank™ access number AF007787). Flanking nucleotides are represented as *smaller letters*, and the 3′ end of the *rep*E gene is represented as an *interrupted boxed arrow*. The position of the maximum of bending induced by RepE is indicated above the sequence by a *hatched rectangle*. Data concerning the footprints detected on the top strand and bottom strand are represented above and below the sequence, respectively. As indicated on the left of the figure, DNaseI and OP-Cu footprints are represented as *double-headed arrows*; *solid lines* indicate the regions strongly (>40%) protected from cleavage by the nucleases on supercoiled or linear DNA, whereas *dashed lines* indicate extended and weaker footprints observed only on supercoiled DNA at high RepE concentration. The *two black ovals* indicate the sites of DNaseI increased sensitivity at two G residues on the bottom strand on supercoiled DNA (only one hypersensitive G was detected when a linear DNA fragment was used). *Light gray open circles* represent the very weak protection of the G residues against DMS methylation. The *black* and *gray triangles* indicate marked or slight increases of DMS sensitivity, respectively, induced by RepE. The *black bars* indicate the location of the modifications probed by $KMnO_4$ *in vitro* and *in vivo* (their height being proportional to the intensity of modification).

double-stranded origin). We may thus wonder about the function of the high affinity for ssDNA observed with RepE. No ATP binding motifs are present in RepE sequence, and no ATPase activity was detected (data not shown). We propose that RepE binding to ssDNA shifts the equilibrium from a closed to an open complex. The shift requires appropriate superhelicity and the AT-richness of the 3′-end of the origin. The lack of multiple RepE binding sites on double-stranded origin and of a strong RepE-mediated bending may be compensated by its high ssDNA binding activity.

An interplay between RepE and Transcription at the Initiation Step—In initiator-dependent replicons, open complex for-

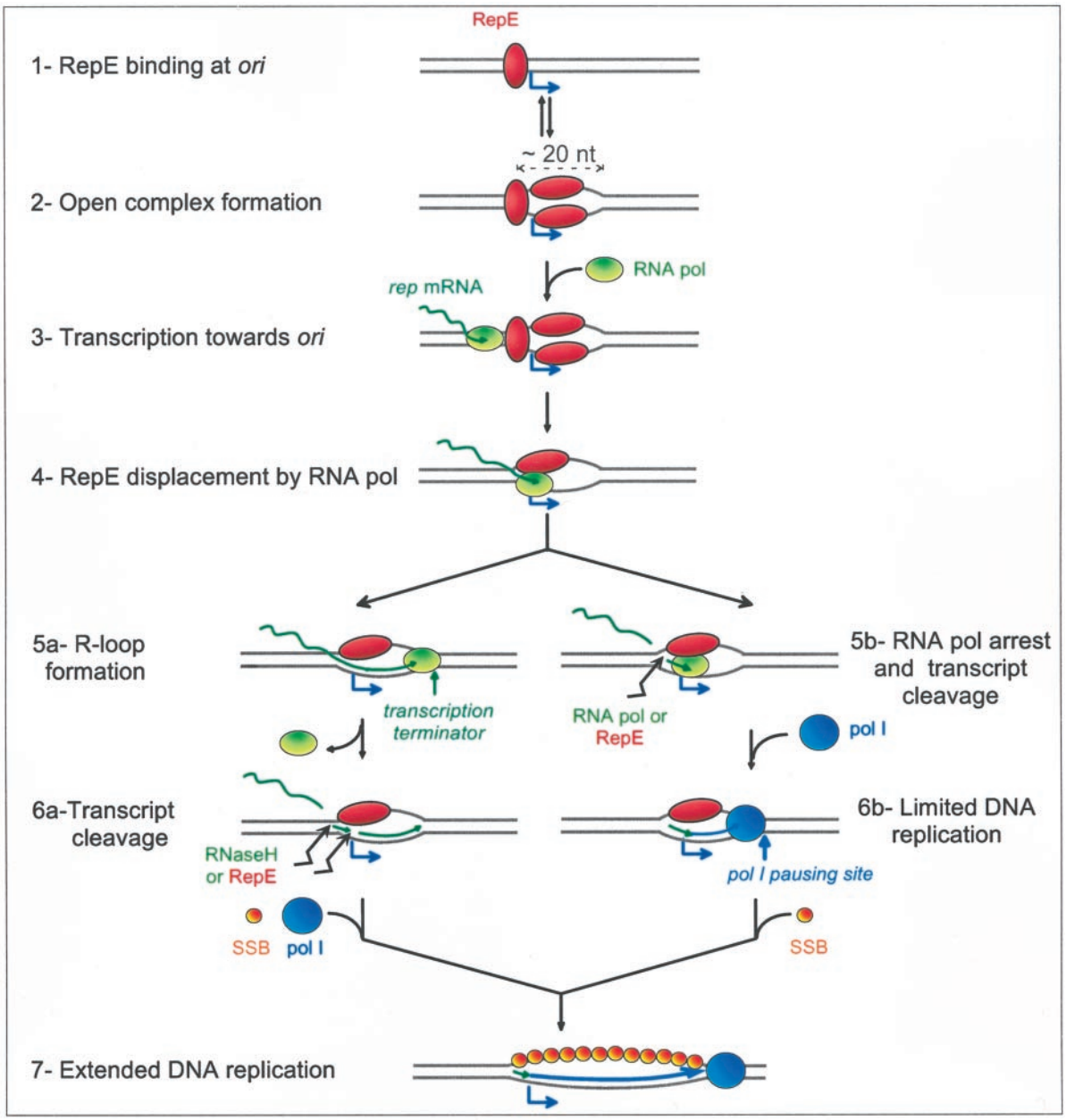

FIG. 11. **Proposed role for RepE in pAMβ1 initiation.** Successive steps of pAMβ1 initiation are indicated, with two alternative pathways (*a* and *b*) proposed for primer generation. See text for details.

mation is required for loading the replicative helicase and polymerase. In pAMβ1, this function is fulfilled by the PriA-dependent primosome loaded on nascent D-loop replication intermediates generated by Pol I (31–33).[2] Thus, all the data obtained in this work and that previously published lead us to ask the following questions. What is the role of the RepE-mediated open complex formation (Pol I loading is not known to require such opening)? What is the function of the transcription through the origin, which is essential for replication?

The most attractive hypothesis is that (i) transcription through the origin provides a primer for Pol I (since transcripts ending at the initiation site and 10 nt upstream were shown to be generated *in vivo* in a RepE- and *ori*-dependent way (26)), and (ii) the maturation of the transcript requires formation of the RepE-mediated open complex. The model for initiation of pAMβ1 replication is thus the following (Fig. 11). After formation of the open complex (*steps 1–2*), a collision between a transcription fork and RepE takes place (*step 3*). To allow transcription to proceed at least until the initiation site, it is supposed that this collision is followed by displacement of RepE from its dsDNA-binding site and possibly from its bottom strand ssDNA-binding site (*step 4*). We propose that two pathways may then be followed. In the first one (*step 5a*), the RNA pol continues transcription for ~20 nt past the initiation site until it reaches putative transcription terminator. RepE protein bound to the top strand might prevent DNA pairing behind the transcription fork, causing R-loop formation. This accounts for the data obtained in the $KMnO_4$ footprint experiment *in vivo* showing that the bottom strand of the open complex was not modified to the same extent as it was *in vitro*, indicating base pairing of this strand with a nucleic acid (Fig. 7*A* and 10). The RNA strand of the R-loop could then be cleaved at the initiation site and about 10 nt upstream by an RNaseH activity provided either by RepE or by a host-encoded enzyme (*step 6a*). The primer thus generated is then extended by Pol I (*step 7*). In a second pathway (*step 5b*), alternative to R-loop formation, RNA pol stops at the initiation site, and the halted polymerase cleaves the mRNA at position −10, thus producing a 10-nt-long

primer for Pol I. It is known that some proteins bound to DNA are able to arrest RNA pol (RTP/ter (67); DnaA/*dnaA* box (68)). Moreover, pausing of RNA pol has been observed in several systems to activate an RNA pol-linked RNase activity that cleaves the nascent RNA molecule about 10 nt upstream of the pausing site (69). In this hypothesis, RNA pol arrest would be mediated in an uncharacterized way by RepE bound to the ssDNA region of the open complex. To account for the protection of the bottom strand against $KMnO_4$ oxidation observed *in vivo* (Fig. 7*A*), we suggest that a limited DNA synthesis (~20 nt long) must occur in these intermediates (*step 6b*). However, this protection is still detected in a strain lacking the DNA polymerase activity of Pol I. This could be explained by a DNA synthesis due either to residual activity of Pol I remaining in the *polA5* strain or to another DNA polymerase able to replace Pol I for synthesis of the first 20 nt in this strain.

In addition to providing a primer, a possible function of the transcript could also be to assist open complex formation, as observed in other systems (3, 70). Yet this hypothesis seems unlikely since the open complex forms efficiently *in vitro* in the absence of any transcription (even though in λ phage, for example, the requirement for transcription is absolute *in vivo* but not *in vitro* when purified proteins are used (71)). Another argument against transcriptional activation is that *in vivo* the $KMnO_4$ footprint of the open complex is highly similar to that detected *in vitro*, except, as discussed above, for the bottom strand, for which the modified region is narrowed to a few nt preceding the initiation site (see Fig. 7*A* and 10). This result is not compatible with a transitory passing of the transcription bubble, but it rather indicates that a nucleic acid is stably paired to the bottom strand.

Whatever the nucleic acid present in the open complex, the *in vivo* $KMnO_4$ footprinting experiments indicate a striking abundance of these structures (~50% of the molecules are modified by $KMnO_4$). This suggests that these molecules are not true replication intermediates but rather abortive replication products originating from the structures represented Fig. 11, *step 6a* or *6b*. Their abundance is consistent with the strong expression of the *repE* gene (~800 molecules of *repE* mRNA per cell (72)) in the high copy number derivatives of pAMβ1 used in this study.

In conclusion, the experiments reported here reveal unexpected properties of the RepE initiator protein, pointing to an original way of initiating DNA replication. Future work should allow us to describe further the interplay between the RepE activities and origin transcription and, thus, allow us to understand more fully this original initiation mechanism, which is conserved in plasmids harbored very broadly in Gram-positive bacteria.

Acknowledgments—We thank Marie-Françoise Noirot-Gros for performing preliminary experiments of this work and Patrice Polard, Stephen McGovern, and Stéphanie Marsin for extremely useful advice during RepE overproduction and purification as well as for providing help and suggestions during this work. We thank Marie-Agnès Petit for critical reading of the manuscript.

REFERENCES

1. Kaguni, J. M. (1997) *Mol. Cell* **7,** 145–157
2. Mizushima, T. (2000) *J. Biochem. (Tokyo)* **127,** 1–7
3. Bramhill, D., and Kornberg, A. (1988) *Cell* **54,** 915–918
4. Bramhill, D., and Kornberg, A. (1988) *Cell* **52,** 743–755
5. Kim, S., Dallmann, H. G., McHenry, C. S., and Marians, K. J. (1996) *Cell* **84,** 643–650
6. Fang, L., Davey, M. J., and O'Donnell, M. (1999) *Mol. Cell* **4,** 541–553
7. Hiasa, H., and Marians, K. J. (1999) *J. Biol. Chem.* **274,** 27244–27248
8. del Solar, G., Giraldo, R., Ruiz-Echevarria, M. J., Espinosa, M., and Diaz-Orejas, R. (1998) *Microbiol. Mol. Biol. Rev.* **62,** 434–464
9. Khan, S. A., and Chattoraj, D. K. (1998) *Plasmid* **40,** 1–11
10. DePamphilis, M. L. (1996) in *DNA Replication in Eukaryotic Cells* (DePamphilis, M. L., ed) pp. 45–85, Cold Spring Harbor Laboratory, Cold Spring Harbor, NY
11. Zannis-Hadjopoulos, M., and Price, G. B. (1999) *J. Cell. Biochem.* **75;** suppl. 32–33
12. Boulikas, T. (1996) *J. Cell. Biochem.* **60,** 297–316
13. Challberg, M. (1996) in *DNA Replication in Eukaryotic Cells* (DePamphilis, M. L., ed) pp. 721–750, Cold Spring Harbor Laboratory, Cold Spring Harbor, NY
14. Ratnakar, P. V., Mohanty, B. K., Lobert, M., and Bastia, D. (1996) *Proc. Natl. Acad. Sci. U. S. A.* **93,** 5522–5526
15. Lu, Y. B., Datta, H. J., and Bastia, D. (1998) *EMBO J.* **17,** 5192–5200
16. Datta, H. J., Khatri, G. S., and Bastia, D. (1999) *Proc. Natl. Acad. Sci. U. S. A.* **96,** 73–78
17. Borowiec, J. A., Dean, F. B., Bullock, P. A., and Hurwitz, J. (1990) *Cell* **60,** 181–184
18. Lehman, I. R., and Boehmer, P. E. (1999) *J. Biol. Chem.* **274,** 28059–28062
19. Thorner, L. K., Lim, D. A., and Botchan, M. R. (1993) *J. Virol.* **67,** 6000–6014
20. Takechi, S., Matsui, H., and Itoh, T. (1995) *EMBO J.* **14,** 5141–5147
21. Konieczny, I., and Helinski, D. R. (1997) *J. Biol. Chem.* **272,** 33312–33318
22. Kornberg, A., and Baker, T. (1992) *DNA Replication* 2nd Ed., W. H. Freeman and Co., New York, NY
23. Minden, J. S., and Marians, K. J. (1985) *J. Biol. Chem.* **260,** 9316–9325
24. Seufert, W., and Messer, W. (1987) *Cell* **48,** 73–78
25. Bruand, C., Le Chatelier, E., Ehrlich, S. D., and Jannière, L. (1993) *Proc. Natl. Acad. Sci. U. S. A.* **90,** 11668–11672
26. Bruand, C., and Ehrlich, S. D. (1998) *Mol. Microbiol.* **30,** 135–145
27. Ceglowski, P., Lurz, R., and Alonso, J. C. (1993) *FEMS Microbiol. Lett.* **109,** 145–150
28. Espinosa, M., Cohen, S., Couturier, M., del Solar, G., Diaz-Orejas, R., Giraldo, R., Jannière, L., Miller, C., Osborn, M., and Thomas, C. M. (2000) in *The Horizontal Gene Pool: Bacterial Plasmids and Gene Spread* (Thomas, C. M., ed) pp. 1–47, Harwood Academic Publishers, Amsterdam, NL
29. Bruand, C., Ehrlich, S. D., and Jannière, L. (1991) *EMBO J.* **10,** 2171–2177
30. Dodd, I. B., and Egan, J. B. (1990) *Nucleic Acids Res.* **18,** 5019–5026
31. Bruand, C., Ehrlich, S. D., and Jannière, L. (1995) *EMBO J.* **14,** 2642–2650
32. Jannière, L., Bidnenko, V., McGovern, S., Ehrlich, S. D., and Petit, M. A. (1997) *Mol. Microbiol.* **23,** 525–535
33. Bidnenko, V., Ehrlich, S. D., and Jannière, L. (1998) *Mol. Microbiol.* **28,** 1005–1016
34. Marians, K. J. (2000) *Trends Biochem. Sci* **25,** 185–189
35. Simon, D., and Chopin, A. (1988) *Biochimie* (*Paris*) **70,** 559–566
36. Kim, J., Zwieb, C., Wu, C., and Adhya, S. (1989) *Gene* **85,** 15–23
37. Carey, J. (1991) *Methods Enzymol.* **208,** 103–117
38. Sigman, D. S., Kuwabara, M. D., Chen, C. H., and Bruice, T. W. (1991) *Methods Enzymol.* **208,** 414–433
39. Sasse-Dwight, S., and Gralla, J. D. (1991) *Methods Enzymol.* **208,** 146–168
40. te Riele, H., Michel, B., and Ehrlich, S. D. (1986) *EMBO J.* **5,** 631–637
41. Dickerson, R. E. (1999) in *Oxford Handbook of Nucleic Acid Structure* (Neidle, S., ed) pp. 145–197, Oxford Science, Oxford
42. Wu, H. M., and Crothers, D. M. (1984) *Nature* **308,** 509–513
43. Hayatsu, H., and Ukita, T. (1967) *Biochem. Biophys. Res. Commun.* **29,** 556–561
44. Rubin, C. M., and Schmid, C. W. (1980) *Nucleic Acids Res.* **8,** 4613–4619
45. Borowiec, J. A., Zhang, L., Sasse-Dwight, S., and Gralla, J. D. (1987) *J. Mol. Biol.* **196,** 101–11
46. Ide, H., Kow, Y. W., and Wallace, S. S. (1985) *Nucleic Acids Res.* **13,** 8035–8052
47. Borowiec, J. A., and Hurwitz, J. (1988) *EMBO J.* **7,** 3149–3158
48. Maxam, A. M., and Gilbert, W. (1977) *Proc. Natl. Acad. Sci. U. S. A.* **74,** 560–564
49. Melnikova, A. F., Beabealashvilli, R., and Mirzabekov, A. D. (1978) *Eur. J. Biochem.* **84,** 301–309
50. Giraldo, R., and Diaz, R. (1992) *J. Mol. Biol.* **228,** 787–802
51. Serrano, M., Salas, M., and Hermoso, J. M. (1990) *Science* **248,** 1012–1016
52. Yang, J., and Carey, J. (1995) *Methods Enzymol.* **259,** 452–468
53. Rice, P. A. (1997) *Curr. Opin. Struct. Biol.* **7,** 86–93
54. Schaper, S., and Messer, W. (1995) *J. Biol. Chem.* **270,** 17622–17626
55. Giraldo, R., Andreu, J. M., and Diaz-Orejas, R. (1998) *EMBO J.* **17,** 4511–4526
56. Kowalski, D., and Eddy, M. J. (1989) *EMBO J.* **8,** 4335–4344
57. Mukhopadhyay, G., Carr, K. M., Kaguni, J. M., and Chattoraj, D. K. (1993) *EMBO J.* **12,** 4547–4554
58. Mukherjee, S., Patel, I., and Bastia, D. (1985) *Cell* **43,** 189–197
59. Zahn, K., and Blattner, F. R. (1987) *Science* **236,** 416–422
60. Mukhopadhyay, G., and Chattoraj, D. K. (1993) *J. Mol. Biol.* **231,** 19–28
61. Snyder, M., Buchman, A. R., and Davis, R. W. (1986) *Nature* **324,** 87–89
62. Eckdahl, T. T., and Anderson, J. N. (1990) *Nucleic Acids Res.* **18,** 1609–1612
63. Learn, B. A., Um, S. J., Huang, L., and McMacken, R. (1997) *Proc. Natl. Acad. Sci. U. S. A.* **94,** 1154–1159
64. Auborn, K. J., Markowitz, R. B., Wang, E., Yu, Y. T., and Prives, C. (1988) *J. Virol.* **62,** 2204–2208
65. Mouw, M., and Pintel, D. J. (1998) *Virology* **251,** 123–131
66. Lee, D. G., Makhov, A. M., Klemm, R. D., Griffith, J. D., and Bell, S. P. (2000) *EMBO J.* **19,** 4774–4782
67. Mohanty, B. K., Sahoo, T., and Bastia, D. (1996) *EMBO J.* **15,** 2530–2539
68. Konopa, G., Szalewska-Palasz, A., Schmidt, A., Srutkowska, S., Messer, W., and Wegrzyn, G. (1999) *FEMS Microbiol. Lett.* **174,** 25–31
69. Eick, D., Wedel, A., and Heumann, H. (1994) *Trends Genet* **10,** 292–296
70. Mensa-Wilmot, K., Carroll, K., and McMacken, R. (1989) *EMBO J.* **8,** 2393–2402
71. Mensa-Wilmot, K., Seaby, R., Alfano, C., Wold, M. C., Gomes, B., and McMacken, R. (1989) *J. Biol. Chem.* **264,** 2853–2861
72. Brantl, S., and Wagner, E. G. (1996) *J. Mol. Biol.* **255,** 275–288
73. Thompson, J. F., and Landy, A. (1988) *Nucleic Acids Res.* **16,** 9687–9705